Electronic Supplementary Information (ESI)

Charge-Order-Induced Directional Enhancement of Non-Diagonal Second-Order Nonlinear Optical Tensor Components

Zuju Ma,[a] Zehui Fang,[a] Zhenlong Xie,[a] Jia-Xiang Zhang,*[,b,c] and Hua Lin,*[,b]

[a]*School of Environmental and Materials Engineering, Yantai University, Yantai, 264005, China*

[b]*State Key Laboratory of Structural Chemistry, Fujian Institute of Research on the Structure of Matter, Chinese Academy of Sciences, Fuzhou 350002, China*

E-mail: linhua@fjirsm.ac.cn and jiaxiangzhang25@stu.pku.edu.cn

[c]*School of Materials Science and Engineering, Peking University, Beijing 100871, China*

Contents

1. Calculation Method

We performed first-principles calculations on the Ag_2BiO_3 using the Projector

Augmented Wave (PAW) method, which is implemented in the Vienna Ab-initio Simulation Package (VASP) [1-5]. For the treatment of exchange-correlation (XC) interactions, we employed three different XC functionals, including the Perdew-Burke-Ernzerhof (GGA-PBE) [6] functional and the Heyd-Scuseria-Ernzerhof hybrid functionals (HSE03 and HSE06) [7]. The HFSCREEN parameter in the distance-separation mixing functionals was set to 0.3 in HSE03 and 0.2 in HSE06, while the default value of AEXX was set at 0.25. Due to quasiparticle self-energy effects, the band gap calculated using the GGA-PBE functional is often smaller than the actual value, leading to overestimations of nonlinear optical polarizability and dielectric constants. To address the underestimation of the band gap, the hybrid HSE03 and HSE06 functional were employed for more accurate results. The valence states were assigned 4d and 5s for Ag, 2s and 2p for O, 6s and 6p for Bi, 5s and 5p for Sb, and 6s and 5d for Ta were used. During the electronic structure calculations, we employed a 7×7×5 Monkhorst-Pack k-point grid. Throughout all calculations, the energy convergence criterion was set to 10^{-4} eV, and the plane-wave cutoff energy was set to 450 eV. The computational settings for $AgGaS_2$ involved structural optimization yielding lattice parameters of a=b=5.829 Å and c=10.539 Å, with electronic and optical properties calculated using a 7×7×4 k-point grid and 200 bands.

The linear optical properties are determined by its complex dielectric function, which consists of the real part $\varepsilon_1(\omega)$ and the imaginary part $\varepsilon_2(\omega)$, expressed as $\varepsilon_1(\omega) = \varepsilon_1(\omega) + i\varepsilon_2(\omega)$.[8] The imaginary part was calculated from direct interband transitions using the Fermi golden rule,[9-10] while indirect transitions were omitted due to their

negligible contribution to ε.

$$\varepsilon_2(\omega) = \frac{4\pi^2 e^2}{\Omega} \lim_{q \to 0} \frac{1}{q^2} \times \sum_{c,\upsilon,\kappa} 2w_k \delta(\mathrm{E}_c - \mathrm{E}_\upsilon - \omega) |\langle c \,|\, e \cdot q \,|\, \upsilon \rangle|^2 \#(1)$$

Where, c and υ denote the integrated optical transitions from the valence states to the conduction states, e is the polarization direction of the photon, and q is the electron momentum operator. The integration over κ is carried out by summing over special k-points with their corresponding weighting factors w_k. The real part of the dielectric function, $\varepsilon_1(\omega)$, is obtained from the imaginary part, $\varepsilon_2(\omega)$, based on the usual Kramers–Kronig transformation.[11]

$$\varepsilon_1(\omega) = 1 + \frac{2}{\pi} \mathrm{P} \int_0^\infty \frac{\varepsilon^{(2)}_{\alpha\beta}(\omega') \omega'}{\omega^2 - \omega^2 + i\eta} d\omega' \#(2)$$

Where, P represents the principal value and η is the complex shift parameter.

The $\chi^{(2)}$ coefficients were calculated within the length-gauge formalism derived by Aversa and Sipe[12] and subsequently modified by Rashkeev *et al*[13]. We employed the computational code developed by Zhang et al.[14], which has been successfully applied to evaluate the second-order susceptibility of various semiconductors and insulators.[15-16] A scissor operator has been added to correct the conduction band energy (corrected to the HSE03 gap)

In the static case, the second-order optical susceptibility can be expressed as:

$$\chi^{abc} = \frac{e^3}{\hbar^2 \Omega} \sum_{nml,k} \frac{r^a_{nm}\left(r^b_{ml} r^c_{ln} + r^c_{ml} r^b_{ln}\right)}{2\omega_{nm}\omega_{ml}\omega_{ln}} [\omega_n f_{ml} + \omega_m f_{ln} +$$

$$+ \frac{ie^3}{4\hbar^2 \Omega} \sum_{nm,k} \frac{f_{nm}}{\omega^2_{mn}} \left[r^a_{nm}\left(r^b_{mn;c} + r^c_{mn;b}\right) + r^b_{nm}\left(r^a_{mn;c} + r^c_{mn;a}\right) + r^c_{nm}(\right.$$

where r is the position operator, $\hbar\omega_{nm} = \hbar\omega_n - \hbar\omega_m$ is the energy difference for the

bands m and n, $f_{mn} = f_m - f_n$ is the difference of the Fermi distribution functions, subscripts a, b, and c are Cartesian indices, and $r^b_{mn;a}$ is the so-called generalized derivative of the coordinate operator in k space,

$$r^{\ b}_{nm;a} = \frac{r^{\ a}_{nm}\Delta^{\ b}_{mn} + r^{\ b}_{nm}\Delta^{\ a}_{mn}}{\omega_{nm}} + \frac{i}{\omega_{nm}} \times \sum_l \left(\omega_{lm} r^{\ a}_{nl} r^{\ b}_{lm} - \omega_{nl} r^{\ b}_{nl} r^{\ a}_{lm}\right) \#(4)$$

where $\Delta^a_{nm} = (p^a_{nn} - p^a_{mm}) / m$ is the difference between the electronic velocities at the bands n and m.

For an external radiation electric field E, the dipole moment μ_i of a group can be expressed as a Taylor series expansion.

$$\mu_i = \mu_i^0 + \alpha_{ij}E_j + \frac{1}{2!}\beta_{ijk}E_jE_k + \frac{1}{3!}\gamma_{ijkl}E_jE_kE_l \qquad (5)$$

where i, j, k, and l subscripts represent the different Cartesian coordinate components x, y, or z. μ_i^0 is the permanent dipole moment of a group, namely the dipole moment without an applied electric field. Physical quantities α, β, and γ correspond to the linear polarizability (α, which corresponds to the linear optical coefficient of a group), first-order hyperpolarizability tensor (β, which is the second-order nonlinear optical coefficient of a group), and second-order hyperpolarizability tensor (γ, which is the third-order nonlinear optical coefficient of a group).

We calculate the static linear polarizability (α) and static first-order hyperpolarizability (β) of [BiO_6], [AgO_3] and [AgO_2] groups in per unit cell of Ag_2BiO_3 at the PBE1PBE level [17] of theory with a reasonably large basis set def2TZVP [18-19] by using the Gaussian 09 program [20]. The polarizability

anisotropy ($\Delta\alpha$) was obtained by the following formula to reflect the sources of birefringence.

$$\Delta\alpha = \sqrt{\left[(\alpha_{xx} - \alpha_{yy})^2 + (\alpha_{xx} - \alpha_{zz})^2 + (\alpha_{yy} - \alpha_{zz})^2\right]/2} \quad (6)$$

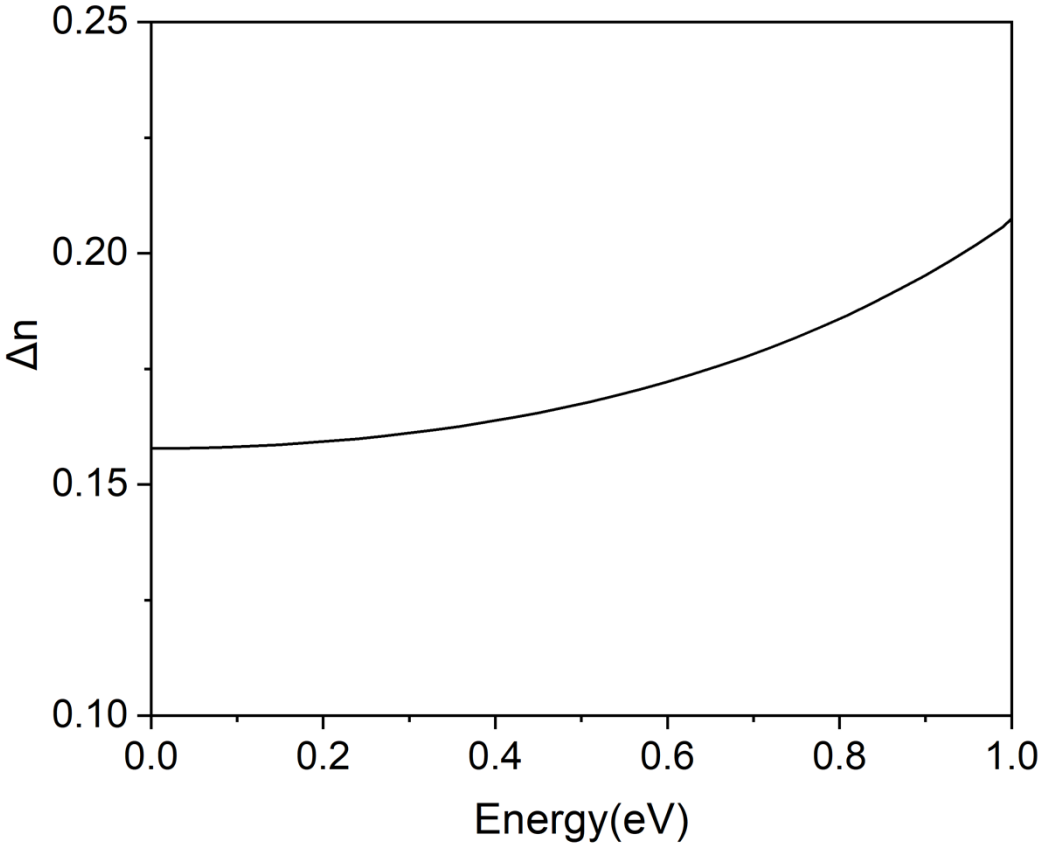

Figure S1. Birefringence *Δn* of Ag_2BiO_3 versus photon energy.

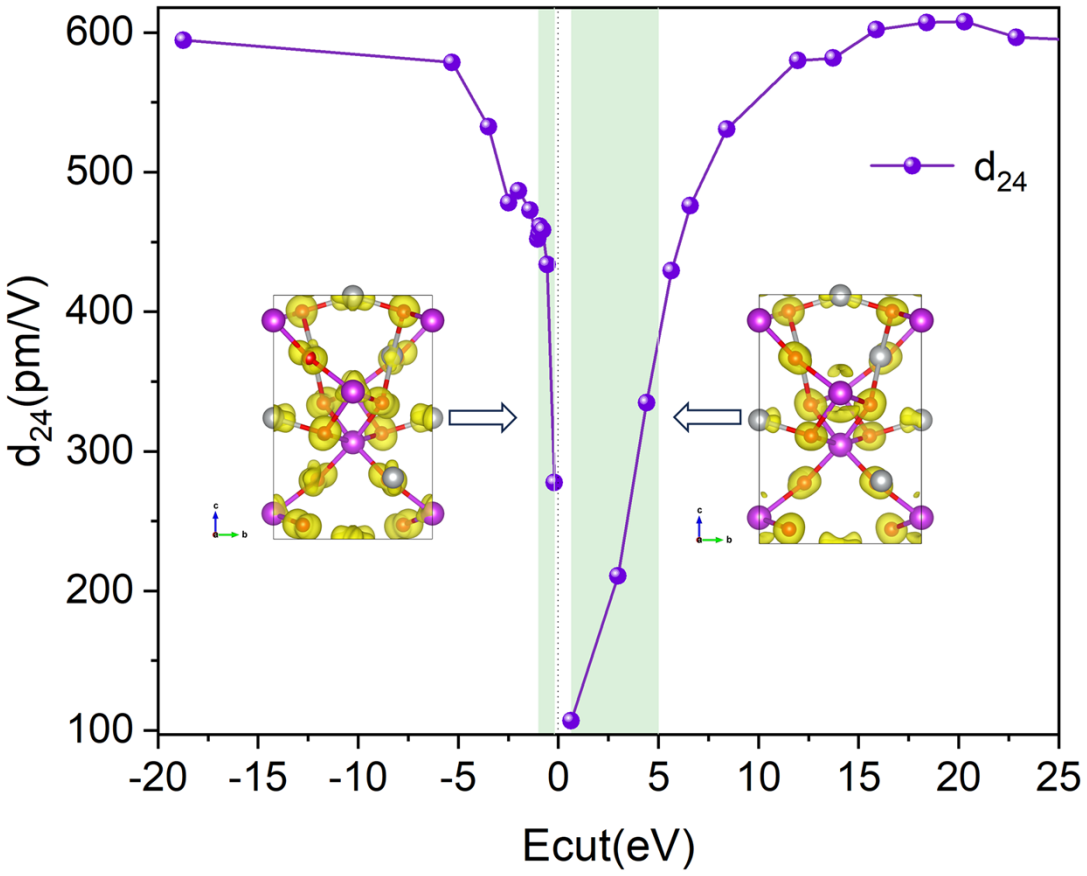

Figure S2. The cutoff-energy-dependent static SHG coefficients $|d_{24}|$ of Ag_2BiO_3.

Table S1. The local dipole moment (μ) in Debye, Linear polarizability α in 10^{-24} esu, Polarizability anisotropy $\Delta\alpha$, and First hyperpolarizability β in 10^{-30} esu for $[BiO_6]$, $[AgO_3]$ and $[AgO_2]$ groups in per unit cell of Ag_2BiO_3.

Groups	Dipole momenta			Linear polarizability α							First hyperpolarizabilityβ		
	x	y	z	Δα	xx	yx	yy	zx	zy	zz	x	y	z
$[Bi^{5+}O_6]$-1	0	0	-0.48	19.41	14.81	-6.91	32.31	0	0	25.56	-0.01	0	-197.44
$[Bi^{5+}O_6]$-3	0	0	-0.48	19.41	14.81	6.91	32.31	0	0	25.56	0	0	-197.44
$[Bi^{3+}O_6]$-2	0	0	0.88	8.67	19.82	-0.3	29.1	0	0	21.26	0	0	108.68
$[Bi^{3+}O_6]$-4	0	0	0.88	8.67	19.82	0.3	29.1	0	0	21.26	0	0	108.68
$[AgO_3]$-1	-0.83	-0.49	0.59	3.75	10.69	-0.27	6.61	-0.45	0.47	8.3	9.45	1.13	-0.1
$[AgO_3]$-2	0.83	0.49	0.59	3.75	10.69	-0.27	6.61	0.45	-0.47	8.3	-9.44	-1.15	-0.09
$[AgO_3]$-3	-0.83	0.49	0.59	3.75	10.69	0.27	6.61	-0.45	-0.47	8.3	9.44	-1.15	-0.09
$[AgO_3]$-4	0.83	-0.49	0.59	3.75	10.69	0.27	6.61	0.45	0.47	8.3	-9.45	1.13	-0.1
$[AgO_2]$-1	0.16	0.02	0.03	15.61	7.45	-2.71	20.74	-0.82	4.18	8.18	-1.58	-0.19	-0.33
$[AgO_3]$-2	-0.16	-0.02	0.03	15.61	7.45	-2.71	20.74	0.82	-4.18	8.18	1.58	0.19	-0.33
$[AgO_3]$-3	0.16	-0.02	0.03	15.61	7.45	2.71	20.74	-0.82	-4.18	8.18	-1.58	0.19	-0.33
$[AgO_3]$-4	-0.16	0.02	0.03	15.61	7.45	2.71	20.74	0.82	4.18	8.18	1.58	-0.19	-0.33

Table S2. The different system of Bi site substitution for Ag_2BiO_3 and their optical components.

System	E_g (eV)	Δn	SHG d_{max} (pm/V)
Ag_2BiO_3	0.87	0.158	d_{24} = 594.57
$Ag_2Bi_{0.75}Sb_{0.25}O_3$	1.12	0.151	d_{24} = 203.58
$Ag_2Bi_{0.5}Sb_{0.5}O_3$	2.3	0.084	d_{33} = 15.06
$Ag_2Bi_{0.75}Ta_{0.25}O_3$	1.03	0.265	d_{24} = 286.49

Reference

1. Blöchl, P. E., Projector augmented-wave method. *Physical review B* **1994,** *50* (24), 17953.

2. Ma, Z.; Hu, J.; Sa, R.; Li, Q.; Zhang, Y.; Wu, K., Screening novel candidates for mid-IR nonlinear optical materials from I_3–V–VI_4 compounds. *Journal of Materials Chemistry C* **2017,** *5* (8), 1963-1972.

3. Koç, H.; Mamedov, A. M.; Deligoz, E.; Ozisik, H., First principles prediction of the elastic, electronic, and optical properties of Sb_2S_3 and Sb2Se3 compounds. *Solid State Sciences* **2012,** *14* (8), 1211-1220.

4. Kresse, G.; Joubert, D., From ultrasoft pseudopotentials to the projector augmented-wave method. *Physical review B* **1999,** *59* (3), 1758.

5. Ceperley, D. M.; Alder, B. J., Ground state of the electron gas by a stochastic method. *Physical review letters* **1980,** *45* (7), 566.

6. Heyd, J.; Scuseria, G. E.; Ernzerhof, M., Hybrid functionals based on a screened Coulomb potential. *The Journal of chemical physics* **2003,** *118* (18), 8207-8215.

7. Monkhorst, H. J.; Pack, J. D., Special points for Brillouin-zone integrations. *Physical review B* **1976,** *13* (12), 5188.

8. Yang, C.-Y.; Zhang, R., First-principles study of the structural, elastic, and optical properties for $Sr_{0.5}Ca_{0.5}TiO_3$. *Chinese Physics B* **2013,** *23* (2), 026301.

9. Li, J.; Duan, C.-g.; Gu, Z.-q.; Wang, D.-s., Linear optical properties and multiphoton absorption of alkali halides calculated from first principles. *Physical Review B* **1998,** *57* (4), 2222.

10. Guo, G.; Chu, K.; Wang, D.-s.; Duan, C.-g., Linear and nonlinear optical properties of carbon nanotubes from first-principles calculations. *Physical Review B* **2004,** *69* (20), 205416.

11. Gajdoš, M.; Hummer, K.; Kresse, G.; Furthmüller, J.; Bechstedt, F., Linear optical properties in the projector-augmented wave methodology. *Physical review B* **2006,** *73* (4), 045112.

12. Aversa, C.; Sipe, J. E., Nonlinear optical susceptibilities of semiconductors: Results with a length-gauge analysis. *Physical Review B* **1995,** *52* (20), 14636.

13. Rashkeev, S. N.; Lambrecht, W. R.; Segall, B., Efficient ab initio method for the calculation of frequency-dependent second-order optical response in semiconductors. *Physical Review B* **1998,** *57* (7), 3905.

14. Fang, Z.; Lin, J.; Liu, R.; Liu, P.; Li, Y.; Huang, X.; Ding, K.; Ning, L.; Zhang, Y., Computational design of inorganic nonlinear optical crystals based on a genetic algorithm. *CrystEngComm* **2014,** *16* (46), 10569-10580.

15. Tang, H.-X.; Zhang, Y.-X.; Zhuo, C.; Fu, R.-B.; Lin, H.; Ma, Z.-J.; Wu, X.-T., A Niobium Oxyiodate Sulfate with a Strong Second-Harmonic-Generation Response Built by Rational Multi-Component Design. *Angewandte Chemie International Edition* **2019,** *58* (12), 3824-3828.

16. Yang, Y.-C.; Liu, X.; Lu, J.; Wu, L.-M.; Chen, L., $[Ag(NH_3)_2]_2SO_4$: A Strategy for the Coordination of Cationic Moieties to Design Nonlinear Optical Materials. *Angewandte Chemie International Edition* **2021,** *60* (39), 21216-21220.

17. Adamo, C.; Barone, V., Toward reliable density functional methods without adjustable parameters: The PBE0 model. *The Journal of chemical physics* **1999,** *110* (13), 6158-6170.

18. Weigend, F.; Ahlrichs, R., Balanced basis sets of split valence, triple zeta valence and quadruple zeta valence quality for H to Rn: Design and assessment of accuracy. *Physical Chemistry Chemical Physics* **2005,** *7* (18), 3297-3305.

19. Weigend, F., Accurate Coulomb-fitting basis sets for H to Rn. *Physical Chemistry Chemical Physics* **2006,** *8* (9), 1057-1065.

20. M. J. Frisch, G. W. Trucks, H. B. Schlegel, G. E. Scuseria, M. A. Robb, J. R. Cheeseman, G. Scalmani, V. Barone, G. A. Petersson, H. Nakatsuji, X. Li, M. Caricato, A. Marenich, J. Bloino, B. G. Janesko, R. Gomperts, B. Mennucci, H. P. Hratchian, J. V. Ortiz, A. F. Izmaylov, J. L. Sonnenberg, D. Williams-Young, F. Ding, F. Lipparini, F. Egidi, J. Goings, B. Peng, A. Petrone, T. Henderson, D. Ranasinghe, V. G. Zakrzewski, J. Gao, N. Rega, G. Zheng, W. Liang, M. Hada, M. Ehara, K. Toyota, R. Fukuda, J. Hasegawa, M. Ishida, T. Nakajima, Y. Honda, O. Kitao, H. Nakai, T. Vreven, K. Throssell, J. A. Montgomery, Jr., J. E. Peralta, F. Ogliaro, M. Bearpark, J. J. Heyd, E. Brothers, K. N. Kudin, V. N. Staroverov, T. Keith, R. Kobayashi, J. Normand, K. Raghavachari, A. Rendell, J. C. Burant, S. S. Iyengar, J. Tomasi, M. Cossi, J. M. Millam, M. Klene, C. Adamo, R. Cammi, J. W. Ochterski, R. L. Martin, K. Morokuma, O. Farkas, J. B. Foresman, and D. J. Fox, Gaussian 09, Revision A.02, Gaussian, Inc., Wallingford CT, **2016.**